Received: 14 September 2021 | Revised: 21 November 2021 | Accepted: 25 November 2021

DOI: 10.1002/app.52003

ARTICLE

Applied Polymer SCIENCE WILEY

Preparation of an oxyalkylated lignin-g-polylactic acid copolymer to improve the compatibility of an organosolv lignin in blended poly(lactic acid) films

Qiang Gu[1,2] | Thomas L. Eberhardt[3] | Jingjing Shao[1,2] | Hui Pan[1,2]

[1]Jiangsu Province Key Laboratory of Green Biomass-based Fuels and Chemicals, Nanjing Forestry University, Nanjing, China

[2]Jiangsu Co-Innovation Center of Efficient Processing and Utilization of Forest Resources, College of Chemical Engineering, Nanjing Forestry University, Nanjing, China

[3]Forest Service USDA, Forest Products Laboratory, Madison, Wisconsin, USA

Correspondence
Hui Pan, Jiangsu Province Key Laboratory of Green Biomass-based Fuels and Chemicals, Nanjing Forestry University, Nanjing, 210037, China.
Email: hpan@njfu.edu.cn

Funding information
National Natural Science Foundation of China

Abstract

To improve the compatibility of an organosolv lignin (OL) in polylactic acid (PLA) blends, a green approach was pursued whereby the lignin was modified with propylene carbonate (PC) to increase its aliphatic hydroxyl content, and thereby, its reactivity. The oxyalkylated organosolv lignin (OOL, synthesized at 170 C) was analyzed by quantitative ^{31}P NMR and showed the number of phenolic hydroxyls decreased from 4.73 to 0.16 mmol g ^{1}, and the number of aliphatic hydroxyls increased from 3.56 to 3.92 mmol g ^{1}. OOL-g-PLA copolymer (OOLPC) samples were prepared by graft polymerization of L-lactide with the OOL and showed the molecular weights (M_n) to range from 12,343 to 16,834 Da, increasing with the lignin loading of the copolymer. Scanning electron microscope indicated that the graft copolymerization reaction between L-lactide and the OOL afforded a copolymer that was compatible with PLA. The highest increase in elongation at break was 7.43% for the PLA blend films prepared with the OOLPC having a 5.0% loading of OOL; the tensile strength at this level of lignin loading was 12.03% lower. Introducing an OL into the blend films showed excellent ultraviolet absorption ability and thus the OOLPC could be used as a well-dispersed UV-blocking agent for biocompatible packaging materials.

KEYWORDS

biocompatibility, copolymers, grafting, membranes

1 | INTRODUCTION

The widespread consumption of conventional plastics has brought about serious environmental concerns, among them being that nondegradable waste plastics now threaten the health of humanity.[1] There is an emerging trend to increase the use of bio-based polymers as a replacement for persistent fossil-based polymers.[2] Progress has been made on the development of cost-effective and environmentally-friendly green materials to replace conventional plastics; however, many of the alternatives still require property improvements to gain widespread use, and there remain opportunities to develop underutilized bio-based polymers. An example of the latter is provided by lignin, the second largest renewable and biodegradable biopolymer after cellulose, that is available as a by-product of the paper/pulp industry, and more recently, biofuel generation. Even today, lignin is still used for its heat value, simply combusted to generate electricity. Therefore, to improve the sustainable development and viability of biomass utilization, it is necessary to investigate economically efficient methods of lignin valorization, one of these being its incorporation into bio-based plastics.

Lignin is a cross-linked phenolic biopolymer material having desirable properties such as UV absorption, antioxidant activity, biodegradability, and flame retardancy.[3,4] Lignin can be cracked and converted to bio-oil fuels and basic chemical feedstocks by thermochemical conversions such as pyrolysis and oxidation.[5,6] Due to lignin is rich in reactive moieties such as phenolic and aliphatic OH groups, it is a viable candidate for the preparation of green polymer materials.[7] Lignin can be used as a feedstock for the preparation of bio-based phenolic resins, polyurethane foams and epoxy resins.[8] In addition, lignin can also be used in the preparation of materials such as fuel cells,[9] carbon fibers,[10] thermoplastics,[11] and polymer films.[12,13]

Polylactic acid (PLA), a thermoplastic polymer made by ring-opening polymerization of lactide or condensation of lactic acid monomers is an important sustainable polymer material.[1] However, its high production cost and some undesirable properties, including brittleness, poor heat resistance, limited gas barrier properties, and poor UV barrier properties, can limit its application. Compared with pure PLA, blends have better thermal stability and constant mechanical strength.[14] In recent years, there have been many reports on blends of lignin with PLA, with the aims of improving and enhancing the properties of PLA materials and/or reducing production costs. Some researchers have prepared lignin-PLA composites with different functions, high impact strength, good thermal stability, antistatic properties and/or biodegradability by directly mixing lignin with PLA[15–17] or adding other materials such as PP.[18] Acetylation[19] or esterification modification with maleic anhydride[20] can improve lignin compatibility with PLA. These blends show better thermal stability and constant mechanical strength compared to pure PLA; however, the problem of poor compatibility of lignin with PLA is not completely solved with these blends.

Self-aggregation of lignin and the high molecular weight of PLA can lead to the compatibility issues between these polymers. Graft copolymerization is considered as one of the most effective methods for lignin modification,[21] and specifically, by graft copolymerization with L-lactide, stable covalent bonds can be formed to improve the adhesion and dispersion of lignin in PLA matrices. Thus, lignin-g-PLA copolymers have been synthesized to improve the compatibility of lignin with PLA. For example, the researchers graft polymerization of lactide onto modified lignins, catalyzed by triazabicyclodecene, gave lignin-PLA materials with enhanced UV absorption and reduced brittleness.[22] After plasma-induced grafting of a pyrolysis-derived lignin with polylactide chains, Dick et al.[23] found that compared with lignin and lignin-g-PLA copolymer, the modification of the lignin particles with the plasma treatment provided the best reinforcement of lignin-PLA composites. Alternatively, Kai et al.[24] prepared different alkylated lignin-g-PLA copolymers by an addition of dodecane to the lignin and then ring-opening polymerization to obtain lignin-PLA electrospun nanofibers with good antioxidant activity and biocompatibility, however, the incorporation of lignin-g-PLA copolymers did not enhance the mechanical properties of the nanofibrous composites. The addition of dodecane to lignin was also used by Ren et al.[7] to prepare alkylated lignin-g-PLA copolymers for toughening PLA; the lignin-PLA blends prepared by mixing the copolymers and PLA showed better UV light blocking, ductility, Young's modulus, and tensile strength. Altogether, studies have shown that the addition of an lignin-g-PLA copolymer to PLA has great potential for expanding the applications for PLA.

The grafting efficiency of aliphatic OH groups of lignin is higher compared to phenolic hydroxyl groups of lignin, and there is preferential grafting to aliphatic OH groups added to lignin.[7,22,25] In this study, we first increased the number of aliphatic OH groups in lignin by oxyalkylation of an organosolv lignin (OL) with propylene carbonate (PC). This step improved the reactivity and accessibility of the OL for polymerization with L-lactide that was carried out to obtain oxyalkylated organosolv lignin-g-PLA copolymer (OOLPC) samples. Finally, these copolymers were blended with PLA to prepare copolymer-PLA blends that were made into films for testing. The effects of the OOLPC properties on the mechanical and optical properties of the copolymer-PLA blend films were then analyzed.

2 | MATERIALS AND METHODS

2.1 | Materials

An OL (M_n = 828 g/mol) was previously produced in the laboratory by the microwave-assisted pretreatment of poplar wood with a methanol/dioxane binary solvent system as described in Zhang et al..[26] PLA (PLA 2003D with MFI of 6 g/10 min) was supplied by Nature Works and L-lactide (99% purity) was kindly provided by Tianjin Exceedbio Technology Co., Ltd. PC and 1,8-diazabicyclo[5.4.0]undec-7-ene (DBU) were purchased from Aladdin Industrial Co.; 2-chloro-4,4,5,5-tetramethyl-1,3,2-dioxa-phospholane (TMDP) was purchased from Sigma-Aldrich.

2.2 | Synthesis of OOLs

OL (5.0 g, 8.3 mmol OH g^{-1}), PC (66 ml), and DBU (0.59 ml) were combined in a screw-cap pressure-resistant vessel (350 ml) that was purged with N_2, sealed, and the contents then magnetically stirred (3 h), heating

at different temperatures (130, 150, 170, and 190 C) using an oil bath. After completing the reaction for a given temperature, the resultant solution was precipitated by pouring over an excess of deionized water. The precipitated OOL was collected on filter paper by vacuum filtration, washed three times with deionized water, and then freeze-dried. Analysis of the OOLs by FTIR spectroscopy showed increased oxyalkylation with increased temperature. Given the similarity in the spectra for the OOLs produced at the two highest temperatures (170 and 190 C), the OOL produced at 170 C, hereafter identified as OOL, was selected for subsequent copolymer syntheses.

2.3 | Synthesis of OOL-g-PLA copolymers

OOL (0.01 g), L-lactide (0.99 g) and DBU (0.05 g) were combined in a screw-cap pressure-resistant vessel (35 ml) that was purged with N_2, sealed, and the contents then magnetically stirred (3.5 h), heating at 130 C using an oil bath. The reaction was quenched with acetic acid followed by precipitation over an excess of methanol to obtain an OOL-g-PLA copolymer (OOLPC) with 1 wt% OOL, identified as $OOLPC_1$. The precipitated copolymer was collected on filter paper by vacuum filtration and then dried in a vacuum oven at 50 C for 24 h. Four additional copolymers with 5, 10, 15, and 20 wt% of OOL were prepared according to the above experimental procedure and identified as $OOLPC_5$, $OOLPC_{10}$, $OOLPC_{15}$, and $OOLPC_{20}$, respectively.

2.4 | Characterization of lignins and copolymers

Fourier transform infrared (FT-IR) spectroscopy was performed on a FTIR spectrometer (Nicolet 380, Thermo Electron) from 4000 to 800 cm ^{1} at a resolution of 4 cm ^{1} and 32 scans per sample. Gel permeation chromatography (GPC) was conducted to determine the molecular weight distributions of the OL, OOL, and OOLPC samples. In each case, a 0.02 g sample was dissolved in tetrahydrofuran (THF) and analyzed following the method described by Hu et al.[27] using a GPC instrument (Waters 1550–2410 system) equipped with Styragel HR1 and HR2 columns (300 mm 718 mm) held at a constant temperature of 35 C. The mobile phase was THF using a flow rate of 1.0 ml/min. ^{1}H NMR spectroscopy of the OOL and OOLPC samples was performed after dissolving each sample (0.03 g) in $CDCl_3$ (0.60 ml). The spectra were measured with a Bruker Avance NEO 400 MHz spectrometer. The number-average molecular weight (M_n) of each grafted PLA chain on the OOLPC samples was calculated using the method of Chung et al.[22] with the following equation:

$$Mn = 72 \quad \frac{H_A}{H_B} + 73 \qquad (1)$$

where H_A is the integrated area of the peaks of PLA at 5.3–5.1 ppm, and H_B is the integrated peak area for the hydrogen atom on the PLA end group at 4.4–4.3 ppm. ^{31}P NMR spectroscopy was performed using a Bruker AVANCE III HD 600 MHz spectrometer according to the procedure in Hu et al.[25] The calculation of hydroxyl group concentration was based on the integration of the following spectral regions: aliphatic OH (150.8–145.0 ppm), phenolic OH (145.0–144.3 ppm), and carboxylic acids (135.6–134.0 ppm). TMDP was used as phosphitylation reagent and cholesterol served as the internal standard (IS) for the quantitative measurements. Samples (0.04 g) of OL and OOL were dissolved in $CDCl_3$/pyridine (1.6/1.0, v/v, 0.5 ml). After the lignin sample was fully dissolved, 0.2 ml N-hydroxy-5-norbornene-2,3-dicarbonylamine solution (9.23 mg/ml) and 0.05 ml chromium acetylacetone solution (5.60 mg/ml), both prepared with $CDCl_3$/pyridine (1.6/1.0, v/v), were added as IS reagent and relaxation reagent, respectively; TMDP (0.10 ml) was then added and the ^{31}P spectrum collected 0.25 h later.

2.5 | Preparation of copolymer-PLA blends

OOL-g-PLA copolymers were mixed with PLA to investigate the properties of copolymer-PLA blends. Each OOL-g-PLA copolymer ($OOLPC_1$, $OOLPC_5$, $OOLPC_{10}$, $OOLPC_{15}$ and $OOLPC_{20}$) and PLA were combined at the ratio of 10:90 (wt: wt) to produce 0.2 g each of blends identified as $OOLPCB_1$, $OOLPCB_5$, $OOLPCB_{10}$, $OOLPCB_{15}$ and $OOLPCB_{20}$, corresponding to the OOLPC used. Copolymer and PLA were combined in a pressure-resistant vessel (75 ml), dissolved in chloroform (10 ml), sealed, magnetically stirred at room temperature for 12 h, and then cast into a flat glass mold to obtain films with a targeted 0.02 mm thickness. After the solvent was evaporated, the films were dried under vacuum at 65 C for 24 h. All film thicknesses were measured with a digital caliper before storing in a desiccator over silica gel.

2.6 | Characterization of copolymer-PLA blends

The scanning electron microscope (SEM) images of the sputter-coated film surfaces were collected with a FEI QUANTA 200 scanning electron microscope with a voltage of 20 kV. Tensile testing was performed on a UTM6503 Electronic Universal Testing Machine from

Shenzhen Suns Technology Stock Co., Ltd., according to China National Standard GB/T 1040.3–2006. Copolymer-PLA blend films (0.02 mm thick) were cut into rectangular specimens (10.0 mm 50.0 mm) and tested with a clamp speed of 5 mm/min. Averages and standard deviations were determined by testing and analyzing five replicate specimens. UV spectra were collected for copolymer-PLA blend films using a PerkinElmer Lambda 950 UV/Vis spectrophotometer in the range of 200 nm to 800 nm at room temperature. UV blocking was calculated with the following equation:

$$\text{Percentage of UV blocking} = 1 \quad T \tag{2}$$

where T is the percentage of UV transmission. Glass transition temperatures (T_g) were measured using differential scanning calorimetry (DSC 214 Polymer) using a heating and cooling rate of 10 C/min. The samples were heated from 25 to 100 C, cooled to 25 C, and heated to 220 C and then kept isothermal for 5 min.

3 | RESULTS AND DISCUSSION

3.1 | Characterization of OOL

To improve the reactivity of the OL, particularly that of the phenolic hydroxyls with L-lactide, it was oxyalkylated with PC. Since the OL used in this study had good solubility in PC, it could be directly modified using PC as the reaction medium. Lignin aromatic and aliphatic OH groups differ in their reactivity with PC with the aliphatic hydroxyls attacking the carbonyl carbon of PC, leading to carbonate linkages, and the aromatic hydroxyls attacking the alkylene carbon, leading to ether linkages (Scheme 1).[28]

The FT-IR spectra of the OOLs synthesized at the different reaction temperatures (130, 150, 170 and 190 C) are shown in Figure 1; the spectrum of the starting OL is provided for comparison. Characteristic bands of lignins are the O-H stretching band (3372 cm ^{1}) and aromatic stretching bands (1594, 1512 and 1425 cm ^{1}), with these bands being present in all the spectra shown. Compared to the OL, slightly more pronounced bands at 2975 and 2935 cm ^{1} can be attributed to the appearance of new C-H stretching of methyl and methylene groups, respectively. The characteristic band at 1260 cm ^{1}, a deformation vibration attributed to the primary and secondary alcohols, is also enhanced for the OOLs; this indicates that the oxyalkylation process was successful for increasing the number of aliphatic OH groups. Another band of interest, a typical carbonate structure C=O bond stretching band at 1740 cm ^{1}, is increased in intensity for the OOLs. Note that the carbonyl stretching vibration peak of PC is at 1794 cm ^{1}, so the possibility of the increased carbonyl peak (1740 cm ^{1}) being residual PC was excluded. Altogether, the reaction of the hydroxyl groups on an OL with PC was successful, and largely increased with the reaction temperature.

Based on the similarity of the FT-IR results for the OOLs produced at the two highest temperatures (170 and 190 C), the lower of these temperatures was deemed sufficient, and therefore the OOL synthesized at 170 C (abbreviated as OOL throughout) was selected for further characterization and use in the copolymer syntheses. The absolute contents of aliphatic OH groups, phenolic OH groups, and carboxyl groups (mmol g ^{1}) in the OOL were determined using quantitative ^{31}P NMR spectroscopy and compared with the pre-modified OL. As shown in Figure 1b, the IS signal peak at 152.0 ppm, along with spectral ranges of 150.8–145.0, 144.3–137.2, and 135.6–134.0 ppm, were used to quantify the aliphatic OH, phenolic OH and carboxyl groups, respectively. In the spectrum of the OOL, the phenolic OH group signals at 144.3–137.2 ppm are absent, indicating that the phenolic OH groups on the OL had reacted with PC during the oxyalkylation reaction. A new peak (146.5–145.0 ppm) appeared within the 150.8–145.0 ppm range for aliphatic OH groups and is assigned to the aliphatic OH groups obtained after the reaction with PC.

Since the peak intensity of the original aliphatic OH group in the OL was weakened, it appears that some aliphatic OH groups had also reacted with the PC. The content of each hydroxyl group was obtained by integration of the spectra, giving the results shown in Table 1. The phenolic OH content decreased from 4.73 to 0.16 mmol g ^{1} and the aliphatic OH content increased from 3.56 to 3.92 mmol g ^{1}. The total number of hydroxyl groups was reduced. Kühnel et al.[28] reported two possible side reactions to account for this, and a concomitant increase in molecular weight; these were an ester exchange reaction between the ester group of the OOL and lignin hydroxyl groups, and a reaction of terminal carbonate structures with hydroxyl groups of the OOL. Altogether, the results showed that lignin polyols were formed, having mostly aliphatic OH groups available for the OOL-g-PLA copolymer (OOLPC) syntheses.

3.2 | Characterizations of the OOL-g-PLA copolymers

Ring-opening polymerizations of different ratios of OOL with L-lactide were then carried out to form a series of OOLPCs. The FTIR spectra of the OOLPCs, and the starting OOL for comparison, are presented in Figure 2a. The OH absorption band (3374 cm ^{1}) for all the OOLPCs

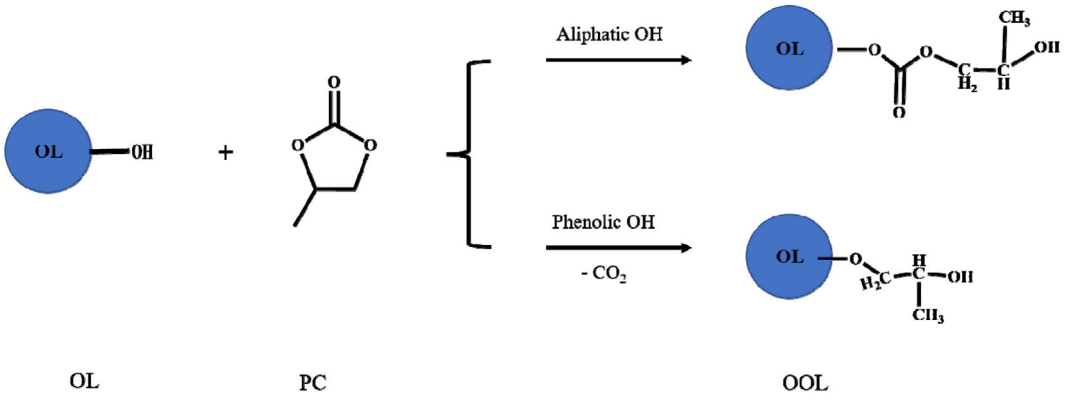

SCHEME 1 Oxyalkylation of organosolv lignin (OL) via propylene carbonate (PC) [Color figure can be viewed at wileyonlinelibrary.com]

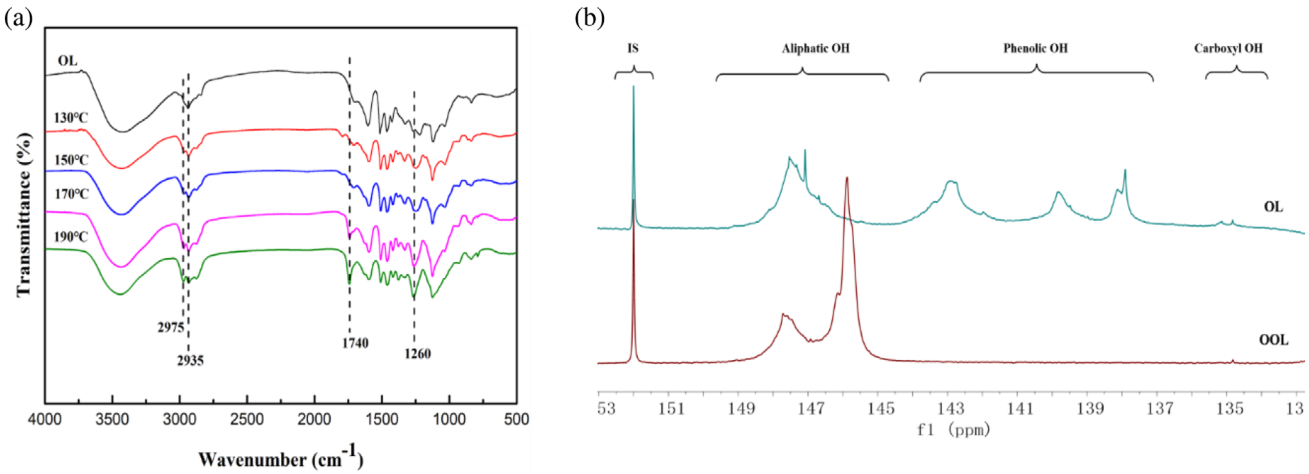

FIGURE 1 (a) Comparison of FT-IR spectra of organosolv lignin (OL) and oxyalkylated organosolv lignins synthesized at different temperatures; (b) The quantitative ^{31}P NMR spectra of OL and OOL, the latter synthesized at 170 C [Color figure can be viewed at wileyonlinelibrary.com]

TABLE 1 Characteristics of organosolv lignin (OL) and oxyalkylated organosolv lignin (OOL)

Sample	Aliphatic OH (mmol g 1)	Phenolic OH (mmol g 1)	Carboxylic OH (mmol g 1)	Total OH (mmol g 1)
Organosolv lignin	3.56	4.73	0.02	8.30
Oxyalkylated organosolv lignin	3.92	0.16	0.01	4.09

is significantly weaker compared to that of the OOL. This is attributed to the OOL hydroxyl group consumption in the ring-opening polymerization with the L-lactide cross-ester. The methyl and methylene absorption bands at 2998 and 2948 cm 1, respectively, are attributed to those functionalities inherent to PLA. A new and pronounced band is found in the spectra of the OOLPCs at 1756 cm 1; this band is assigned to the asymmetric stretching of C=O in the branched PLA after ring opening polymerization, apart from the much weaker C=O band at 1740 cm 1 for the PC moiety in the OOL. Altogether, these results confirmed the successful preparation of a series of OOLPCs by the ring-opening polymerization with L-lactide.

The chemical functionality of the OOLPCs was further analyzed using ^{1}H NMR to estimate the M_n of the grafted PLA chains (Figure 2b). Compared to the OOL, there are two new peaks of interest in each of the OOLPC

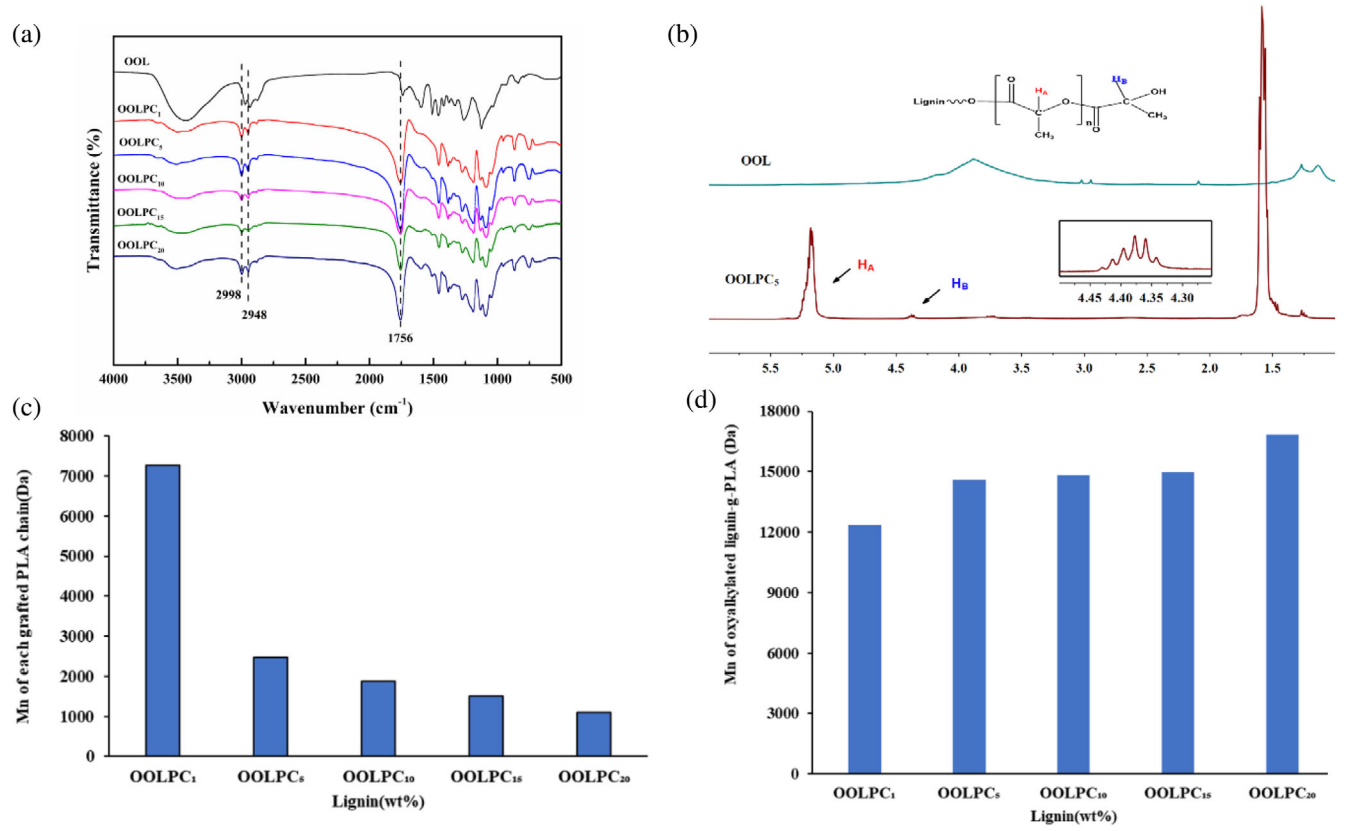

FIGURE 2 (a) Comparison of FT-IR spectra of oxyalkylated organosolv lignin (OOL) and each oxyalkylated organosolv lignin-g-PLA (OOLPC) sample; (b) ^{1}H NMR spectra of OOL and $OOLPC_5$, the signal at 4.4–4.3 ppm is enlarged as inserted image; (c) Number-average molecular weight (M_n) of each grafted PLA chain on the OOLPCs; (d) M_n of OOLPCs [Color figure can be viewed at wileyonlinelibrary.com]

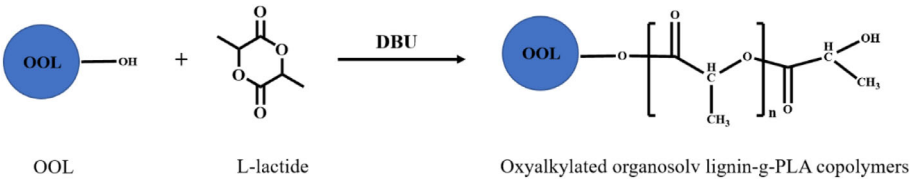

SCHEME 2 Ring-opening polymerization of L-lactide on oxyalkylated organosolv lignin (OOL) [Color figure can be viewed at wileyonlinelibrary.com]

spectra, assigned to protons on the grafted PLA chains per Chung et al.[22] The peaks at 5.3–5.1 ppm are assigned to the recurring unit protons (H_A) on PLA (in Scheme 2) and the small peaks at 4.4–4.3 ppm are assigned to the proton (H_B) on the PLA end group. The signals at 4.0 ppm and 1.5–1.0 ppm in OOL are attributed to a large number of aliphatic OH groups newly generated and new methyl protons after oxyalkylation. After graft copolymerization with L-lactide, the signal at 4.0 ppm disappears, which is due to the reaction of the newly generated aliphatic hydroxyl group with L-lactide,[29] and the signal at 1.5–1.0 ppm does not disappear and is shifted with the grafting of L-lactide. The appearance of the signal at 1.5 ppm is attributed to the hydrogen atoms of methyl in the lactide monomer unit of the PLA grafted chains.[23] Peak integrations were then used in Equation 1 to calculate M_n of the PLA chain (Figure 2c). These results suggested that the average chain length of PLA decreased with each stepwise increase in the proportion of OOL. Thus, with increasing proportions of OOL, there would be higher numbers of hydroxyl groups available to react with the L-lactide, as a competing reaction for the polymerization of L-lactide into PLA chain extensions.

The M_n values of the OOLPCs were then determined by GPC (Figure 2d) and showed them to increase with the increasing proportion of OOL. The lowest M_n for the OOLPCs (12,343 Da) is with the lowest OOL proportion ($OOLPC_1$). The M_n increases to 16,834 Da for the OOLPC with the highest OOL proportion ($OOLPC_{20}$); at the intermediate OOL proportions, the M_n values are essentially the same. These results suggested that with the increase of the amounts of OOL relative to lactide monomer, the

reduced length of the grafted PLA chain was offset by increased lignin crosslinking, resulting in equivalent or higher M_n values for the OOLPCs. Other researcher groups have reported that cyclic PLA was preferentially generated at low lignin loading (5 wt% lignin) and star graft copolymers were generated at higher lignin loadings (≥10 wt%).[30,31] For the lignin-g-PLA star copolymers that were formed, the chain lengths were shorter when generated under the higher lignin loading conditions.

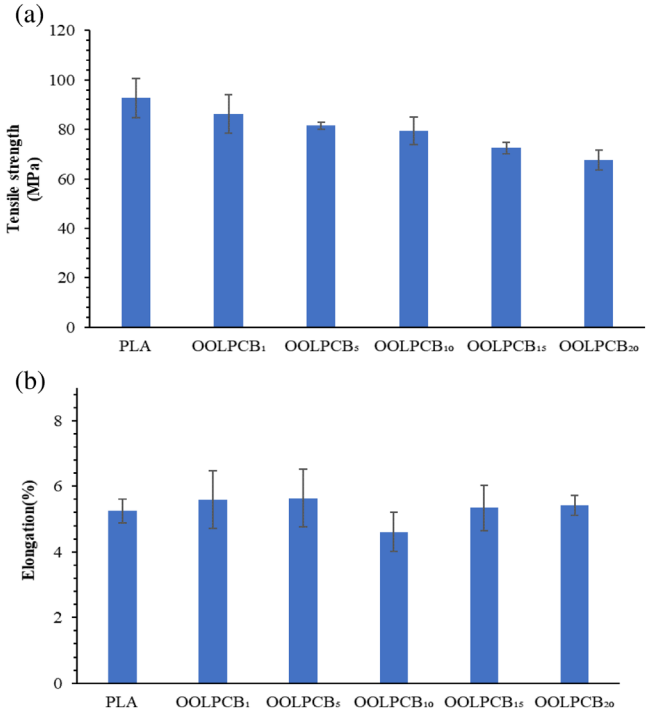

FIGURE 3 Mechanical properties of oxyalkylated organosolv lignin-g-PLA copolymer blend (OOLPCB) samples; error bars show standard deviations of the averages [Color figure can be viewed at wileyonlinelibrary.com]

3.3 | Characterizations of copolymer-PLA blends

Synthesized OOLPCs and a commercial PLA were used to prepare OOLPC-PLA blend (OOLPCB) samples. The results from the tensile testing of the resultant films are shown in Figure 3. Neat PLA exhibits the highest tensile strength (92.62 MPa); its low value for the elongation at break (5.25%) indicated high brittleness.[14] The tensile strength of the OOLPCBs decreased with increased lignin content in the OOLPC. Similarly, Li et al.[32] reported the tensile strength of a lignin-PLA blend was reduced from 68.1 to 48.3 MPa with 10 wt% added lignin; the reductions of the mechanical properties of the blends were attributed to the presence of lignin particles, which prevented the formation of the long-range continuous phase of PLA. OOL-g-PLA copolymers with suitable grafted PLA chain lengths, and if well dispersed, have been reported to be useful as plasticizers for inherently brittle PLA materials.[22] In the current study, the

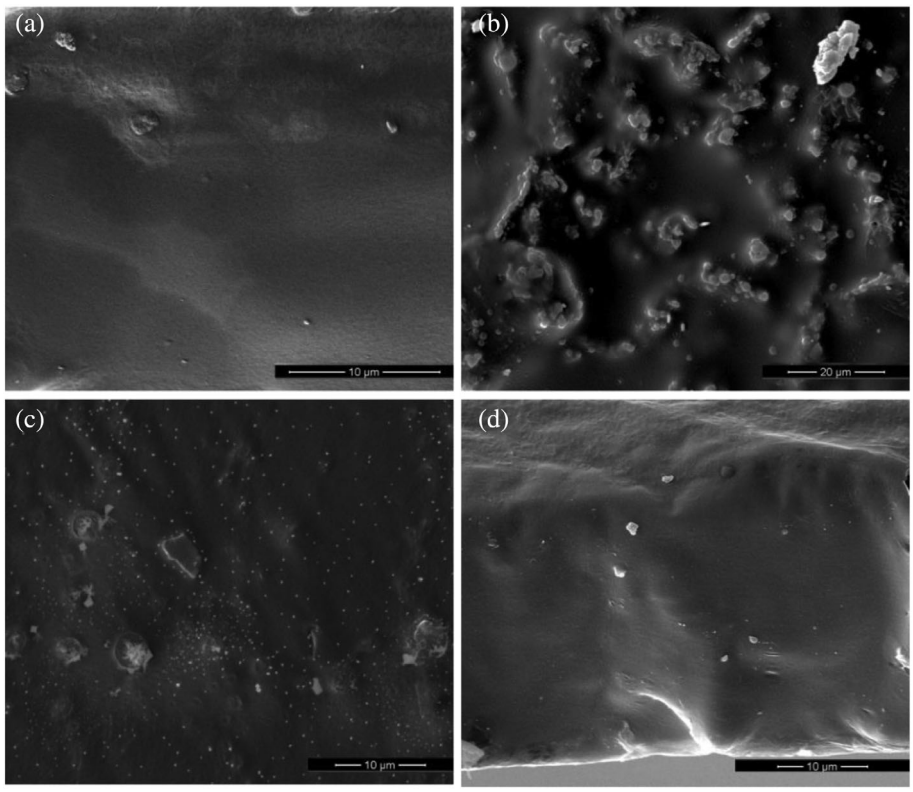

FIGURE 4 Scanning electron microscope (SEM) images of (a) PLA, (b) Organosolv lignin-PLA blend (OLB), (c) Organosolv lignin-g-PLA copolymer-PLA blend (OLPCB), and (d) Oxyalkylated organosolv lignin copolymer-PLA blend ($OOLPCB_5$)

elongation at break results were mixed overall, with no definite increasing or decreasing trend in the values. With the two lowest lignin loadings, the small decrease in tensile strength was offset by small increases in elongation at break. Thus, for the blend with $OOLPC_5$, that being $OOLPCB_5$, the slight decrease in tensile strength from 92.62 to 81.48 MPa (12.03%) was offset by a slight increase in elongation at break from 5.25% to 5.64% (+7.43%).

As stated above, with the higher lignin loadings in the OOLPCs, the lower the tensile strength of resultant PLA blends. Since the copolymer graft chain length (Figure 2c) decreased with increased lignin loading in the copolymer, the decrease in tensile strength may have resulted from lower entanglement of the copolymer PLA chains with bulk PLA. Also, for the lower M_n values, coinciding with the lower copolymer lignin loadings, more uniform dispersion of the copolymer in the PLA matrix should result in tougher blends. Altogether, the addition of OOLPCs to PLA resulted a small decrease in strength, with a small increase in toughness. Therefore, compared to PLA, lignin is less costly and can partially replace PLA without affecting the overall performance to achieve cost reductions.

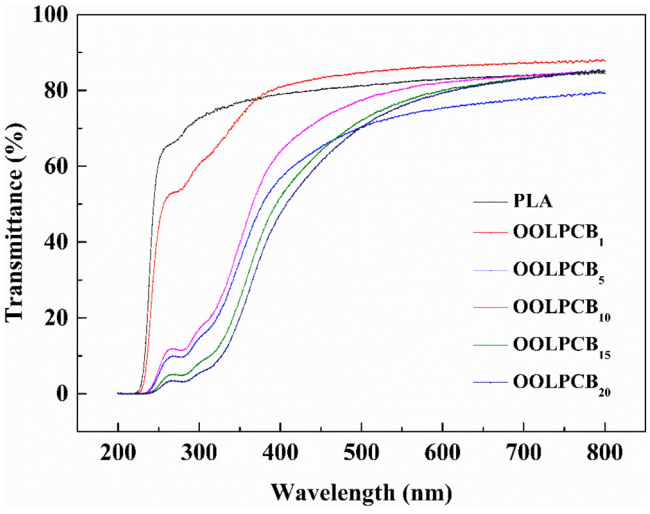

FIGURE 5 Light transmittance of copolymer-PLA blends in the wavelengths of UV and visible light [Color figure can be viewed at wileyonlinelibrary.com]

The surface properties of neat PLA and lignin/PLA films from different blending methods were assessed by SEM characterization and the images are shown in Figure 4a–d. Among the OOLPCBs produced in the current study, $OOLPCB_5$ had the highest elongation at break and was thus selected for imaging by SEM. The neat PLA film demonstrated a smooth surface as shown in Figure 4a. The OLB displays a rough surface with obviously aggregated particles which was due to the poor compatibility of unmodified lignin with PLA (Figure 4b). When unmodified OL grafted with L-lactide before blending with PLA, the resulted OLPCB shows smoother surface than OLB, indicating the improved compatibility by grafting the OL with L-lactide (Figure 4c). The compatibility of lignin/lactide copolymer with PLA was further improve by oxyalkylation modification of lignin before grafting with L-lactide as suggested by the smooth surface of the $OOLPCB_5$ film (Figure 4d). In addition, DSC characterizations of the blends were also performed (Figure S2). The results show that only one glass transition temperature (Tg) and one crystallization melting temperature (Tm) are presented in the DSC curves of all OOL-g-PLA copolymer-PLA blends (Table S1), indicating the modified lignin copolymers showed good compatibility with PLA.

PLA is widely used as a packaging material, but its poor UV resistance limits its applications.[33] By adding lignin, the UV light absorption capacity of lignin-PLA blends can be improved.[34] As shown in Figure 5, the OOLPCB films have a high UV-blocking function yet retain good visible light transmission. Compared with

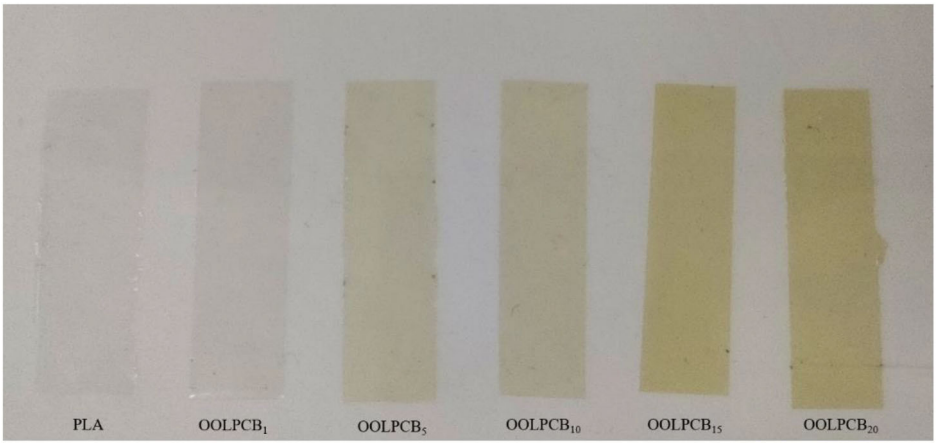

FIGURE 6 Photographs of copolymer-PLA blends ($OOLPCB_1$, $OOLPCB_5$, $OOLPCB_{10}$, $OOLPCB_{15}$ and $OOLPCB_{20}$) [Color figure can be viewed at wileyonlinelibrary.com]

the PLA film, the color of the OOLPCB films gradually became yellow as the OOL content in the OOLPC increased (Figure 6), which is due to the fact that an OOL itself is yellow.[35,36] The UV absorption capacity of the OOLPCB films increased with increased wt% OOL in the OOLPC used for blending. Among the blends, $OOLPCB_5$, prepared by blending PLA with $OOLPC_5$, gave a comparable UV blocking capacity to the blends with higher lignin loadings; $OOLPCB_{20}$ can achieve a maximum 68% UV-C (100–280 nm), 74% UV-B (280–315 nm) and 78% UV-A (315–400 nm) blocking performance.[7] Thus, OOL-g-PLA copolymers can be used as a well-dispersed UV-blocking agent for biocompatible packaging materials.

4 | CONCLUSIONS

In this study, the oxyalkylation of an OL with PC improved the reactivity and accessibility of its hydroxyl groups. With the increase in lignin loading, the length of PLA grafting chains decreased, and the molecular weight of the copolymers increased. The copolymer-PLA blends, prepared by blending PLA with OOL-g-PLA copolymers gave smooth films, as evidenced by SEM. This suggests that the oxyalkylation of the lignin and the graft copolymerization with L-lactide improved its dispersion in PLA. The decrease in tensile strength of the blends with the increase in lignin loading can be attributed to the decrease of the PLA chain length of the OOL-g-PLA copolymers leading to less entanglement of the copolymer PLA chains and bulk PLA. Since the ultraviolet transmittance of the copolymer-PLA blends increased with the increase in lignin loading, even small additions of lignin, as derivatives compatible with PLA, may expand the utility of PLA as a packaging material that provides protection from ultraviolet light.

ACKNOWLEDGMENTS

The authors are grateful for the financial support from National Natural Science Foundation of China (No.31770631).

DATA AVAILABILITY STATEMENT

The data that support the findings of this study are available from the corresponding author upon reasonable request.

ORCID

Hui Pan https://orcid.org/0000-0001-5074-8314

REFERENCES

[1] X. Ge, M. Chang, W. Jiang, B. Zhang, R. Xing, C. Bulin, *J. Appl. Polym. Sci.* **2020**, *137*, 49354.
[2] W. Yang, Y. Weng, D. Puglia, G. Qi, W. Dong, J. M. Kenny, P. Ma, *Int. J. Biol. Macromol.* **2020**, *144*, 102.
[3] B. M. Upton, A. M. Kasko, *Chem. Rev.* **2016**, *116*, 2275.
[4] W. O. S. Doherty, P. Mousavioun, C. M. Fellows, *Ind. Crops Prod.* **2011**, *33*, 259.
[5] S. Laurichesse, L. Avérous, *Prog. Polym. Sci.* **2014**, *39*, 1266.
[6] P. Figueiredo, K. Lintinen, J. T. Hirvonen, M. A. Kostiainen, H. A. Santos, *Prog. Mater. Sci.* **2018**, *93*, 233.
[7] W. Ren, X. Pan, G. Wang, W. Cheng, Y. Liu, *Green Chem.* **2016**, *18*, 5008.
[8] C. C. Xu, L. Dessbesell, Y. Zhang, Z. Yuan, *Biofuels Bioprod. Biorefining* **2021**, *15*, 32.
[9] E. Antolini, *ChemSusChem* **2021**, *14*, 189.
[10] F. Torres-Canas, A. Bentaleb, M. Föllmer, J. Roman, W. Neri, I. Ly, A. Derré, P. Poulin, *Carbon N.Y.* **2020**, *163*, 120.
[11] M. Parit, Z. Jiang, *Int. J. Biol. Macromol.* **2020**, *165*, 3180.
[12] M. Esmaeili, I. Anugwom, M. Mänttäri, M. Kallioinen, *Membranes (Basel).* **2018**, *8*, 80.
[13] A. Sarwono, Z. Man, M. A. Bustam, D. Subbarao, A. Idris, N. Muhammad, A. S. Khan, Z. Ullah, *Environ. Technol. (United Kingdom)* **2018**, *39*, 1522.
[14] O. Gordobil, R. Delucis, I. Egüés, J. Labidi, *Ind. Crops Prod.* **2015**, *72*, 46.
[15] I. Spiridon, K. Leluk, A. M. Resmerita, R. N. Darie, *Compos. Part B Eng.* **2015**, *69*, 342.
[16] A. Duval, M. Lawoko, *React. Funct. Polym.* **2014**, *85*, 78.
[17] T. F. da Silva, F. Menezes, L. S. Montagna, A. P. Lemes, F. R. Passador, *Mater. Sci. Eng. B Solid-State Mater. Adv. Technol.* **2019**, *251*, 114441.
[18] E. Triwulandari, M. Ghozali, D. Sondari, M. Septiyanti, Y. Sampora, Y. Meliana, S. Fahmiati, W. K. Restu, A. Haryono, *Plast. Rubber Compos.* **2019**, *48*, 82.
[19] O. Gordobil, I. Egüés, R. Llano-Ponte, J. Labidi, *Polym. Degrad. Stab.* **2014**, *108*, 330.
[20] I. Anugwom, V. Lahtela, M. Kallioinen, T. Kärki, *Ind. Crops Prod.* **2019**, *140*, 111704.
[21] H. Liu, H. Chung, *J. Polym. Sci. Part A Polym. Chem* **2017**, *55*, 3515.
[22] Y. L. Chung, J. V. Olsson, R. J. Li, C. W. Frank, R. M. Waymouth, S. L. Billington, E. S. Sattely, *ACS Sustainable Chem. Eng.* **2013**, *1*, 1231.
[23] T. Atz Dick, J. Couve, O. Gimello, A. Mas, J. J. Robin, *Polymer (Guildf).* **2017**, *118*, 280.
[24] D. Kai, W. Ren, L. Tian, P. L. Chee, Y. Liu, S. Ramakrishna, X. J. Loh, *ACS Sustainable Chem. Eng.* **2016**, *4*, 5268.
[25] X. Z. M. G. Mcauley, *J. Polym. Chem.* **1994**, *32*, 2965.
[26] Y. Zhang, Z. Wang, J. Feng, H. Pan, *Bioresour. Technol.* **2020**, *300*, 122657.
[27] L. Hu, H. Pan, Y. Zhou, C. Y. Hse, C. Liu, B. Zhang, B. Xu, *J. Wood Chem. Technol.* **2014**, *34*, 122.
[28] I. Kühnel, B. Saake, R. Lehnen, *Ind. Crops Prod.* **2017**, *101*, 75.
[29] I. Kühnel, J. Podschun, B. Saake, R. Lehnen, *Holzforschung* **2015**, *69*, 531.
[30] J. Yu, J. Wang, C. Wang, Y. Liu, Y. Xu, C. Tang, F. Chu, *Macromol. Rapid Commun.* **2015**, *36*, 398.
[31] L. E. Chile, S. J. Kaser, S. G. Hatzikiriakos, P. Mehrkhodavandi, *ACS Sustainable Chem. Eng.* **2018**, *6*, 1650.
[32] J. Li, C. S. Chua, *IEEE Int. Conf. Image Process.* **2003**, *3*, 949.

[33] R. Bhardwaj, A. K. Mohanty, *Biomacromolecules* **2007**, *8*, 2476.
[34] S. Y. Park, J.-Y. Kim, H. J. Youn, J. W. Choi, *Int. J. Biol. Macromol.* **2019**, *138*, 1029.
[35] C. E. Hoyle, A. B. Lowe, C. N. Bowman, *Chem. Soc. Rev.* **2010**, *39*, 1355.
[36] Y. Kim, J. Suhr, H. W. Seo, H. Sun, S. Kim, I. K. Park, S. H. Kim, Y. Lee, K. J. Kim, J. Nam, *Do Sci. Rep.* **2017**, *7*, 43596.

SUPPORTING INFORMATION

Additional supporting information may be found in the online version of the article at the publisher's website.

How to cite this article: Q. Gu, T. L. Eberhardt, J. Shao, H. Pan, *J. Appl. Polym. Sci.* **2022**, *139*(16), e52003. https://doi.org/10.1002/app.52003